

Journal of
Applied Remote Sensing

RemoteSensing.SPIEDigitalLibrary.org

Improving soil moisture retrieval accuracy of Advanced Microwave Scanning Radiometer 2 in vegetated areas using land surface parameters of Visible Infrared Imaging Radiometer Suite

Saeed Arab
Gregory L. Easson

SPIE.

Saeed Arab, Gregory L. Easson, "Improving soil moisture retrieval accuracy of Advanced Microwave Scanning Radiometer 2 in vegetated areas using land surface parameters of Visible Infrared Imaging Radiometer Suite," *J. Appl. Remote Sens.* **13**(4), 044520 (2019), doi: 10.1117/1.JRS.13.044520.

Improving soil moisture retrieval accuracy of Advanced Microwave Scanning Radiometer 2 in vegetated areas using land surface parameters of Visible Infrared Imaging Radiometer Suite

Saeed Arab[†] and Gregory L. Eason*

University of Mississippi, Mississippi Mineral Resources Institute, University,
Mississippi, United States

Abstract. The current remote sensing systems designed to measure soil moisture have a relatively coarse spatial resolution ranging from 25 to 50 km. The Advanced Microwave Scanning Radiometer 2 (AMSR2) is a passive sensor that measures soil moisture through C-band (6.9 and 7.3 GHz) observation of brightness temperature (BT). AMSR2 uses land parameter retrieval model to retrieve surface soil moisture and vegetation optical depth. This model partitions the microwave observation into its respective soil and vegetation emission components. AMSR2 loses sensitivity to soil moisture as vegetation density increases, during the growing season. Field observations show that AMSR2 tends to overestimate the soil moisture when the vegetation intensity increases and covers the soil. We address two existing issues in the use of soil moisture products of the AMSR2: (1) spatial resolution of the soil moisture product and (2) the impact of vegetation cover on the radiative transfer. We used a vegetative index to estimate when soil moisture retrieval is not sufficiently accurate and how the optical data can be used to improve soil moisture estimation. The land surface temperature and vegetation index products of the Visible Infrared Imaging Radiometer Suite are used to downscale the AMSR2 soil moisture products to 1 km. A series of soil moisture data collected in the field were used to analyze the accuracy of the downscaled soil moisture values and the results indicated that introduction of the BT in the downscaling model improves the accuracy of the soil moisture products over the vegetated areas. The mean absolute error (MAE) of the downscaled soil moisture values is ~5.6%—an improvement to 8.0% of original AMSR2 soil moisture products. In the presence of vegetation, however, the MAE is still greater than that of a similar analysis of AMSR2 product over semiarid areas. © 2019 Society of Photo-Optical Instrumentation Engineers (SPIE) [DOI: [10.1117/1.JRS.13.044520](https://doi.org/10.1117/1.JRS.13.044520)]

Keywords: remote sensing; soil moisture; vegetated areas; Advanced Microwave Scanning Radiometer 2.

Paper 190468 received Jun. 20, 2019; accepted for publication Oct. 29, 2019; published online Nov. 22, 2019.

1 Introduction

The volume of water content in the upper layer of soil, soil moisture, is a fundamental controlling variable in many hydrological processes.^{1,2} Soil moisture is one of the main factors in the study of global water, energy, and carbon cycles, as well as watershed applications, such as flood and drought monitoring, water resources management, and crop yield forecasts.³

Microwave remote sensing has demonstrated the ability to map and monitor relative changes in soil moisture over large areas, as well as the opportunity to measure absolute values of soil moisture through inverse models.⁴ Compared to most natural surfaces (e.g., dry soil, rock, or vegetation), the microwave dielectric constant (ϵ_r) of water is high.^{4,5} Because of large differences in the dielectric constant of dry soil and water⁴ and the fact that microwave emissivity

*Address all correspondence to Gregory L. Eason, E-mail: geason@olemiss.edu

[†]Present Address: KBR, Contractor to the U.S. Geological Survey Earth Resources Observation and Science Center, Sioux Falls, South Dakota, United States

of the soil is a function of surface dielectric constant,^{4–6} the variations in surface soil moisture can be studied through microwave reflectivity.⁷ The Fresnel reflection equations are used to predict the surface microwave emissivity as a function of the dielectric constant and the viewing angle (θ) based on the polarization of the sensor.⁸

Despite the developments of soil moisture measurement instruments, current widespread soil moisture products are usually at coarse resolutions ranging from 25 to 50 km with large amounts of uncertainty in the data. The uncertainty of soil moisture data is due to the fact that (1) soil moisture fluctuates spatially and temporally due to the geological and climatic conditions and depends on soil type⁹ and (2) in almost all of the soil moisture-observing instruments, the measured backscatter is a combination of soil and overlying vegetation cover responses, and the vegetation water content contribution increases with increase in vegetation height and its water content.^{10,11}

The emissivity, whether it is the backscatter recorded by a radiometer or the return signal from radar, can be influenced by surface parameters such as roughness, vegetation cover, and soil density/texture.¹² Hence, different models have been developed to account for vegetation and roughness. For remote sensing in the microwave portion, however, only wavelengths greater than ~5 cm are particularly effective, as these wavelengths have fewer problems with interference from the atmosphere and vegetation, sense deeper into the soil, and maximize soil moisture sensitivity.¹³

For bare soil conditions, the emissivity is approximated by dividing the brightness temperature (BT) by the soil effective temperature. In the presence of vegetation, the observed emissivity is a composite of the soil and vegetation, and the vegetation cover characteristics can have a significant impact on the emissivity. The land parameter retrieval model (LPRM), developed by Owe et al.,¹⁴ is based on a radiative transfer model that solves for soil moisture and vegetation optical depth (VOD) simultaneously. The LPRM uses the microwave polarization difference index from passive microwave observations in an analytical approach for the simultaneous VOD estimation. Partitioning of the emissivity into the soil and vegetation components by LPRM has improved the accuracy of soil moisture estimation over the vegetated areas.¹⁵

Soil moisture retrieval over bare and sparsely vegetated areas has been extensively researched and many models have been developed regarding this issue. Soil moisture retrieval over vegetated areas, however, is more complicated because vegetation and surface roughness reduce the sensitivity of microwave observations to soil moisture.^{16,17} During the plant-growing season, as the vegetation cover and its water content increases, the accuracy of soil moisture retrieval using microwave remote sensing significantly decreases.¹⁸ Therefore, the soil moisture-sensing system may reach a point at which estimated values will no longer correlate with the *in-situ* observations.^{19,20}

In this study, the accuracy of soil moisture retrieval over vegetated areas during different plant growth stages is characterized, and a potential method for improving the soil moisture accuracy is proposed. The main objective of this paper is to provide quality assessment of the soil moisture product from Advanced Microwave Scanning Radiometer 2 (AMSR2) as a function of vegetation index (VI). The absolute accuracy of the soil moisture product from the AMSR2 over different crop types is analyzed, and a downscaling method is applied on the AMSR2's C-band radiometer data to improve the accuracy and spatial resolution of the soil moisture product.

2 Data

2.1 Ground-Based Soil Moisture

The *in-situ* soil moisture data were collected at sites in five counties in Mississippi Delta during the plant-growing season of 2016. The main crop types in this region are soybean, cotton, and corn, and there are very few small rice and wheat farms. Figure 1 shows the distribution of the stations that are visited monthly for soil moisture data collection. During the field visits, soil moisture data were collected at 33 stations using a soil moisture probe. In each station, the soil moisture data were collected at several nearby but variant locations and then averaged to include

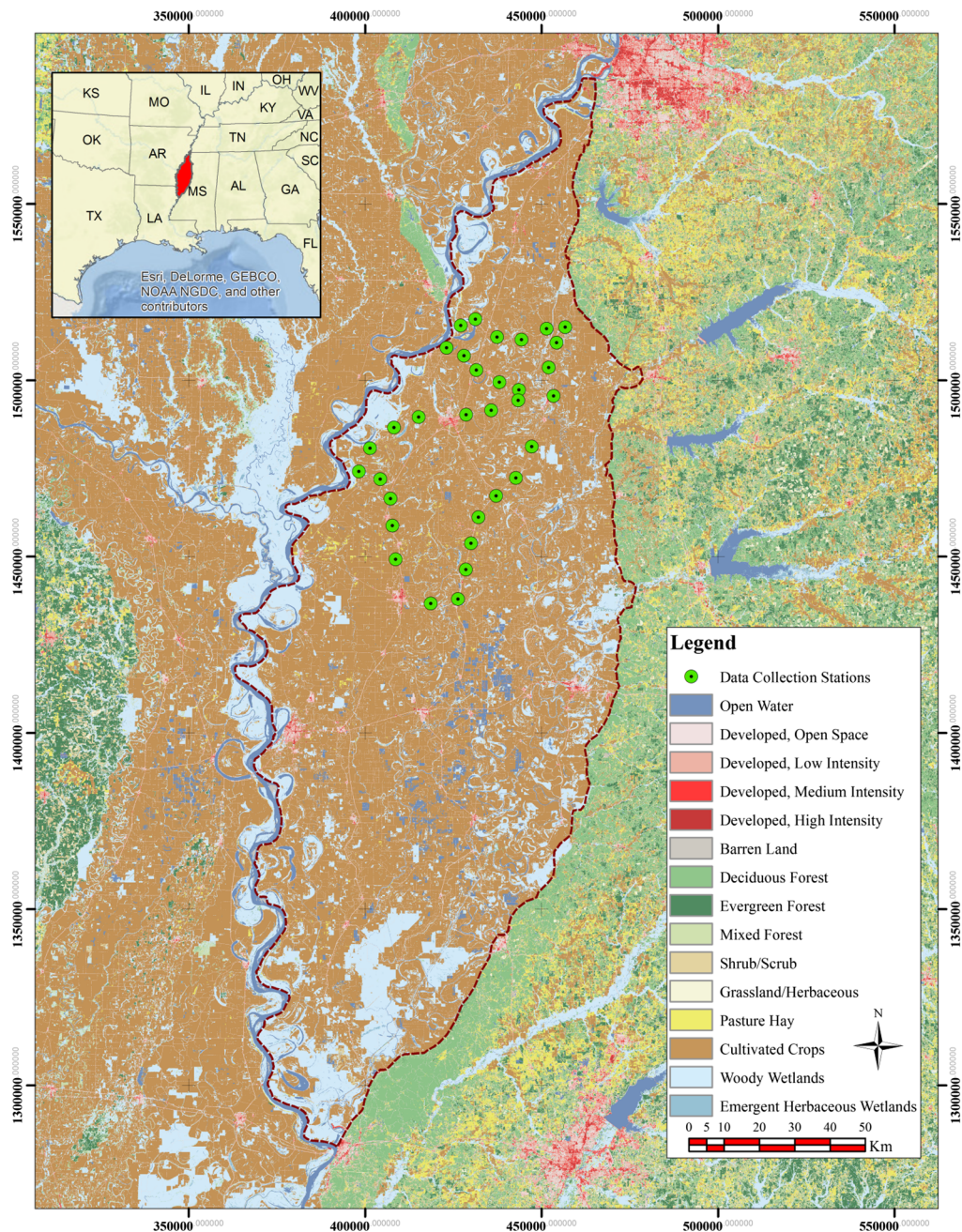


Fig. 1 Study site and data collection stations in the Mississippi Delta. Land cover from National Land Cover Database 2011 (NLCD 2011).²¹

the heterogeneity of the land surface and soil moisture in the satellite pixels. The uniformity of the soil type, elevation, and the land cover within the visited fields guarantees the representativeness of the *in-situ* observations on the scale of satellite pixels.

Microwave BT observation at C-band is sensitive to the soil moisture in top 1 to 2 cm of the soil.²² Therefore, the soil moisture content was measured at the same depth. In this study, a portable Waterscout™ SM100 was used with the Fieldscout® soil sensor reader to measure the volumetric soil moisture information instantaneously. For each measurement, after removing a few centimeters of the soil top, the sensor blade was horizontally pushed in the soil at the depth of ~2 cm and the soil moisture value was recorded. The sensor has the nominal accuracy of 3% in soil moisture measurement at the soil condition with electrical conductivity smaller than 8 millisiemens/cm, which is within the range of electrical conductivity of agricultural fields.²³

Furthermore, at sites where the soil is near its plastic limit, a soil sample was collected for calibration purposes. The gravimetric method described in ASTM D 2216-98 instruction²⁴ was used to calculate the soil moisture content of the samples in the lab to calibrate the soil moisture probe data.

2.2 Visible Infrared Imaging Radiometer Suite Data

Visible Infrared Imaging Radiometer Suite (VIIRS) is a scanning radiometer onboard Suomi National Polar-orbiting Partnership spacecraft that collects visible and infrared imagery and radiometric measurements of land, atmosphere, cryosphere, and oceans. The sensor was successfully launched in October 2011. The VIIRS Environmental Data Record (EDR) products are validated by National Oceanic and Atmospheric Administration (NOAA) Joint Polar Satellite System. As a product validation procedure, both land surface temperature (LST) and vegetation index (VI) EDR products reached stage 1 validation-level maturity in 2014.^{25,26} The spatial resolution of the LST product is 0.75 km at nadir. The VIIRS VI product is generated daily at the resolution of 0.375 km at nadir over land in swath form. VIIRS data were acquired from NOAA Comprehensive Large Array-Data Stewardship System.²⁷ The top of atmosphere—normalized difference vegetation index (NDVI) and LST data that are collected during ascending node (crossing the equator around 13:30 local time) are used in this study.

During the data preparation, the cloud-contaminated pixels within the VIIRS optical dataset were masked. Masking the cloud pixels made it necessary to have alternative data resources for some study dates. Assuming that in the absence of precipitation the change in VI from day to day is negligible, for some study dates the VI data are constructed by substituting masked pixels by VIIRS VI value in the day before/after the study date. For missing LST information, the daily 1-km MYD11 products of the moderate resolution imaging spectroradiometer (MODIS) sensor were used when it was necessary. Aqua MODIS (MYD11) passes over the equator about the same time as VIIRS (13:30).

2.3 Advanced Microwave Scanning Radiometer 2 Data

The AMSR2 sensor onboard Global Change Observation Mission-Water (GCOM-W) is a multichannel microwave radiometer. AMSR2 measures daily global soil moisture and BT data with improved radio frequency interference mitigation, compared to its predecessor the Advanced Microwave Scanning Radiometer for the Earth Observing System.²⁸ Surface soil moisture is derived from BT data using LPRM.²⁸ The LPRM is based on a forward radiative transfer model to retrieve surface soil moisture and VOD. The BT is measured at the frequencies of 6.9, 7.3, 10.6, 18.7, 23.8, 36.5, and 89 GHz. The penetration depth into and through the vegetation canopy is better for low-frequency bands, especially over dense canopies.^{4,29} Therefore, the low-frequency C-bands (6.9 and 7.3 GHz) contain more information about soil emissivity beneath the canopy rather than the emissivity from overlying vegetation canopy. The vertically polarized BT has less dependence on soil roughness and has shown a negative correlation with soil moisture content in arid areas,³⁰ but horizontally polarized BT data are more sensitive to soil moisture variations.⁸ Level-3 soil moisture product of the AMSR2 is available at 10-km grids, which are derived from the nominal 46-km-resolution C-band and 31-km-resolution X-band data using resampling and smoothing filter-based intensity modulation technique.³¹ In this study, the 10-km level-3 H-polarized BT and soil moisture products generated from applying LPRM model on 6.9-GHz band observations are used for the analysis. AMSR2 data were acquired from the Japan Aerospace Exploration Agency GCOM-W1 data-providing service.³²

2.4 Precipitation Data

The precipitation data collected by Soil Climate Analysis Network (SCAN) stations are used for the validation of calculated soil moisture values. The SCAN precipitation data were acquired from National Resources Conservation Service database.³³

3 Data Analysis

The *in-situ*-measured soil moisture data were utilized to assess the accuracy of AMSR2 soil moisture products. The *in-situ* data collected during the different growing stages show the impact of vegetation height and density on the AMSR2 accuracy over the time. Figure 2 shows observed errors in AMSR2 coarse resolution (10-km) soil moisture for major vegetation types in the agricultural fields in the Mississippi Delta. The vertical axis is the difference between *in-situ*-measured soil moisture and AMSR2-estimated soil moisture for the visited data points in major land cover types from April to September 2016 when the vegetation completes one growing cycle. A positive difference (points above horizontal axis) suggests an underestimation, whereas negative difference indicates an overestimation in the AMSR2 soil moisture.

In early stages of the growing season ($0 < \text{NDVI} < 0.4$), the soil moisture estimation accuracy of observed points falls within the standard accuracy of AMSR2 soil moisture product ($\pm 10\%$). However, the negative slopes of the trendlines in Fig. 2 indicate that the difference between *in-situ*-measured and remotely sensed soil moisture increases with NDVI increase over the croplands. Therefore, AMSR2 tends to overestimate the soil moisture as the crops grow and as the vegetation density increases. The linear trendlines of corn and soybean intersect the -10% difference line at NDVI of 0.553 and 0.604, respectively, suggesting that the AMSR2 measurements are not within the standard accuracy limit. Different trendlines are mainly due to different scattering and attenuating properties of the various crop types. Different tillage practices used in corn, soybean, and cotton fields and the roughness effect of the soil on emissivity can also be the reasons for different trendlines. The coefficient of determination (R^2) for corn, cotton, soybean, and uncultivated trendlines are 0.94, 0.07, 0.32, and 0.01, respectively. The higher R^2 value for the corn suggests that the error in AMSR2's estimated soil moisture over this crop type has an inverse linear relationship with NDVI, whereas the sample data collected over other crop types do not indicate a linear relationship with NDVI. The inverse relationship illustrated by trendlines of corn, cotton, and soybean indicates that global constant parameters for the radiative transfer used in this LPRM implementation are not appropriate for these agricultural settings.

Those farms that were being irrigated at the time of field visit and had a high soil moisture value are out of AMSR2 standard accuracy interval (difference $> 10\%$). This is because AMSR2 averages the BT observation over an area of 25×25 km and, depending on the area that is being irrigated, the high soil moisture value in the field might be missing in the coarse-resolution AMSR2 image.

4 Method

In this study, AMSR2 10-km C-band data were downscaled to 1-km resolution using a modified VI-LST model. Downscaling is the process of relating information or data at relatively coarse

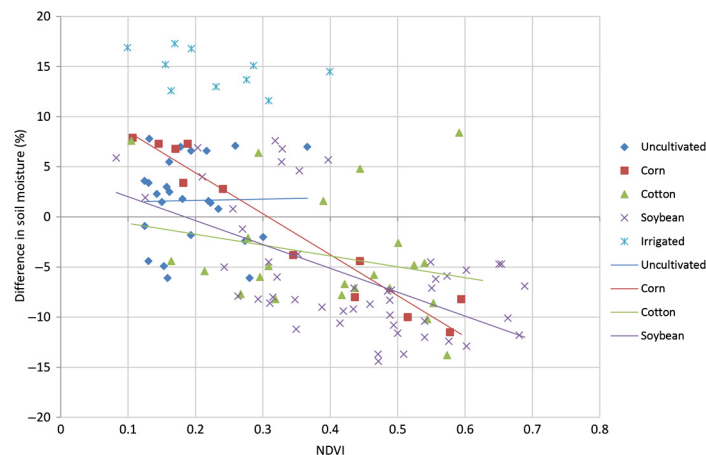


Fig. 2 Difference between soil moisture content measured *in-situ* and estimated by AMSR2 over the agricultural fields of the Mississippi Delta. *In-situ* soil moisture data were collected from April to September 2016.

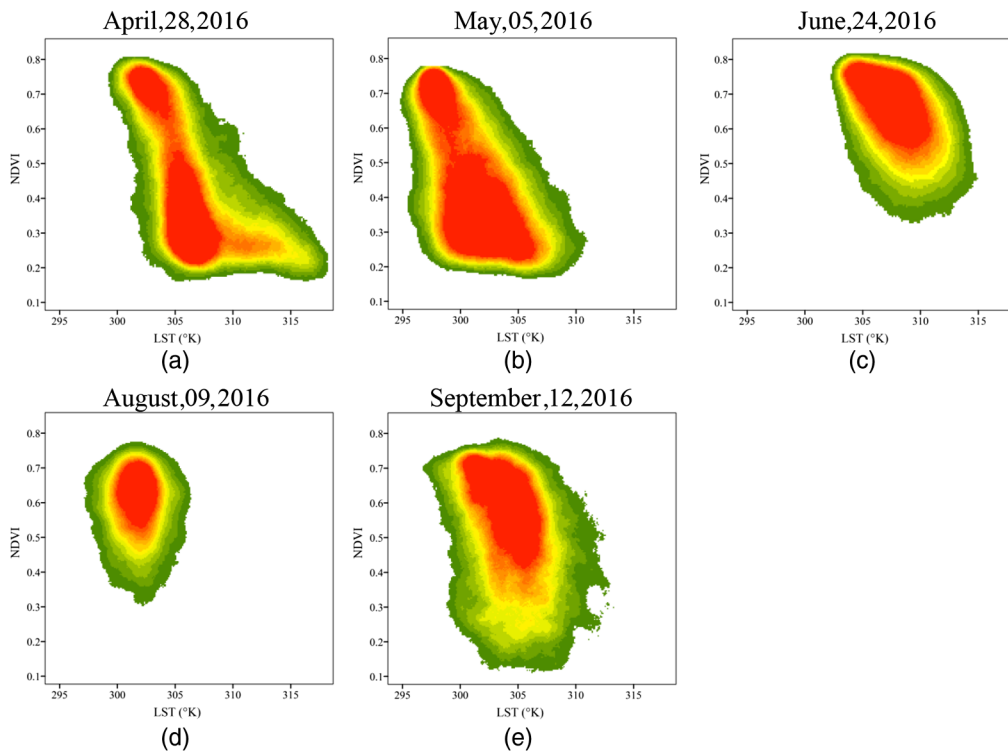


Fig. 3 Heatmap plots of VI-LST for different study dates from April to September 2016. The heatmaps of April 28 and May 5 reveal well-defined triangles.

spatial and temporal scales to desired products at finer spatial and temporal scales. The down-scaling algorithm used in this study is based on the universal triangle concept that relates NDVI and LST to the soil moisture.³⁴

Figure 3 illustrates the heatmap plots of NDVI and LST for the five study dates. In a condition where a large number of pixels reflect a full range of vegetation cover and soil surface wetness, the LST-NDVI scatter plot would resemble a triangle or a trapezoid³⁵ where each border reflects a real physical limit. The lower and upper borders of the triangle reflect bare soil and full vegetation cover, respectively, and the left and slanted right borders indicate lower and upper limits of the surface soil water content, i.e., completely dry or field capacity, respectively.³⁶

The well-defined triangular borders for April and May data [Figs. 3(a) and 3(b)] indicate that all the above-mentioned physical limits had existed in the field when VIIRS imaged the Mississippi Delta. The left edge of the triangle shapes in these two figures is the cold border, which consists of the minimum surface radiant temperature at each given NDVI and corresponds to wettest pixels. The slanted right edge of the triangle is called warm edge and corresponds to driest pixels.³⁶

As the crops mature from April to August and more area become covered with vegetation, the optical sensor would see less bare soil pixels and the triangle loses its lower edge. As Figs. 3(c) and 3(d) indicate, the VI-LST heatmap plots lose the triangular shape, which is due to not having a full range of vegetation cover. As the farmers start to harvest in late August and September, more bare soil signature would be seen by the sensor and the VI-LST heatmap plot will start to regain a triangular shape [Fig. 3(e)].

Theoretical and experimental studies of the VI-LST triangle model have demonstrated that there can be a unique relationship between soil moisture, NDVI, and LST for a given region under specific climatic conditions and land surface types.³⁷ The general relationship can be expressed through a regression formula in which soil moisture is a polynomial function of NDVI and LST, as shown in Eq. (1).

$$SM = \sum_{i=0}^n \sum_{j=0}^n a_{ij} NDVI^i LST^j, \tag{1}$$

where SM is the soil moisture, n is the order of the polynomial, and a_{ij} are the coefficients. Piles et al.³⁷ showed that introducing BT in the equation strengthens the relationship between land surface parameters and soil moisture. Thus, Eq. (1) can be modified to Eq. (2) as

$$SM = \sum_{i=0}^n \sum_{j=0}^n \sum_{k=0}^n a_{ijk} NDVI^i LST^j BT^k. \tag{2}$$

The BT includes information on all parameters that dominate the Earth’s emission at C-band, in addition to soil moisture, e.g., vegetation opacity, vegetation scattering albedo, soil roughness, soil texture, and soil temperature.

To downscale 10-km soil moisture product of AMSR2, the coefficients a_{ijk} in the Eq. (2) were determined using aggregated 10-km NDVI and LST and AMSR2 10-km soil moisture and BT products. Then the model coefficients were applied on 1-km NDVI and LST to calculate soil moisture values at 1-km spatial resolution.

The finer resolution NDVI and LST data of VIIRS were aggregated to 10 km by an averaging filter. In the next step, the maximum and minimum values of LST, NDVI, and BT datasets were determined and these values were used to normalize the data. Equation (3) is used to calculate normalized NDVI ($NDVI_N$), normalized LST (LST_N), and normalized BT (BT_N).

$$\begin{cases} NDVI_N = \frac{NDVI - NDVI_{min}}{NDVI_{max} - NDVI_{min}} \\ LST_N = \frac{LST - LST_{min}}{LST_{max} - LST_{min}} \\ BT_N = \frac{BT - BT_{min}}{BT_{max} - BT_{min}} \end{cases}, \tag{3}$$

where $NDVI_{min}$, $NDVI_{max}$, LST_{min} , and LST_{max} are the minimum and maximum values of aggregated NDVI and LST data and BT_{min} and BT_{max} are minimum and maximum values of the BT dataset.

After substituting normalized values, the expanded form of Eq. (2) will be as follows:

$$\begin{aligned} SM_{AMSR2} = & a_{000} + a_{001}BT_N + a_{010}LST_N + a_{100}NDVI_N \\ & + a_{002}BT_N^2 + a_{020}LST_N^2 + a_{200}NDVI_N^2 + a_{011}LST_N \cdot BT_N \\ & + a_{101}NDVI_N \cdot BT_N + a_{110}NDVI_N \cdot LST_N + \dots \end{aligned} \tag{4}$$

Since normalized parameter values range from 0 to 1, third order and higher terms can be omitted due to their low impact on the result and the equation is approximated to first ten terms.³⁷

Equation (4) can be rewritten in the matrix form of $L = A \times X$ as shown in Eq. (5).

$$\begin{bmatrix} SM_1 \\ SM_1 \\ \vdots \\ SM_n \end{bmatrix} = \begin{bmatrix} 1 & BT_{N_1} & LST_{N_1} & NDVI_{N_1} & BT_{N_1}^2 & LST_{N_1}^2 & NDVI_{N_1}^2 & LST_{N_1} \cdot BT_{N_1} & NDVI_{N_1} \cdot BT_{N_1} & NDVI_{N_1} \cdot LST_{N_1} \\ \vdots & \vdots & \vdots & \vdots & \ddots & \vdots & \vdots & \vdots & \vdots & \vdots \\ 1 & BT_{N_n} & LST_{N_n} & \dots \end{bmatrix} \times \begin{bmatrix} a_{000} \\ a_{001} \\ \vdots \\ a_{110} \end{bmatrix}. \tag{5}$$

The coefficients matrix (a_{ijk}) can be calculated using the least squares theory. Assuming that the matrix $A^T \times A$ is nonsingular, the ordinary least squares estimator for the unknown matrix (X) will be as shown in Eq. (6).³⁸

$$X = (A^T \times A)^{-1} \times A^T \times L. \tag{6}$$

Once the coefficients matrix (X) is calculated, the coefficients are then applied to normalized 1-km LST and NDVI data of VIIRS and the result would be the downscaled soil moisture at 1-km spatial resolution.

5 Results

Microwave remote sensing-derived soil moisture maps at 1 km are generated by applying coefficients a_{ijk} in Eq. (6) to normalized 1-km NDVI and LST data. Figure 4 illustrates the original 10-km soil moisture products of AMSR2 along with 1-km soil moisture maps created using modified universal triangle model. The missing pixels in the downscaled maps are due to cloud masking of VIIRS data.

The patterns of the soil moisture in the agricultural fields of the Mississippi Delta indicate that the distance from the Mississippi River is not as important as the precipitation for the top layer soil moisture. The precipitation data in the days leading up to each study date show how the downscaling model provides more detailed information about soil moisture variation. Figure 5 shows the distribution of the 10 weather stations of the SCAN network within the study site. Figure 6 represents the accumulated precipitation during 5 days prior to each study date in each weather station. For example, in August 9 data, some of the weather stations in western and southern parts of the study site (Scott, Silver City, and Onward) experienced more than 1 inch of rainfall during 5 days before the study date. Compared to the original AMSR2 product that shows high soil moisture concentration for central parts, the downscaled soil moisture map of this date more accurately shows a higher soil moisture values in the southern and western parts of the study site as the result of the precipitation that occurred before data collection.

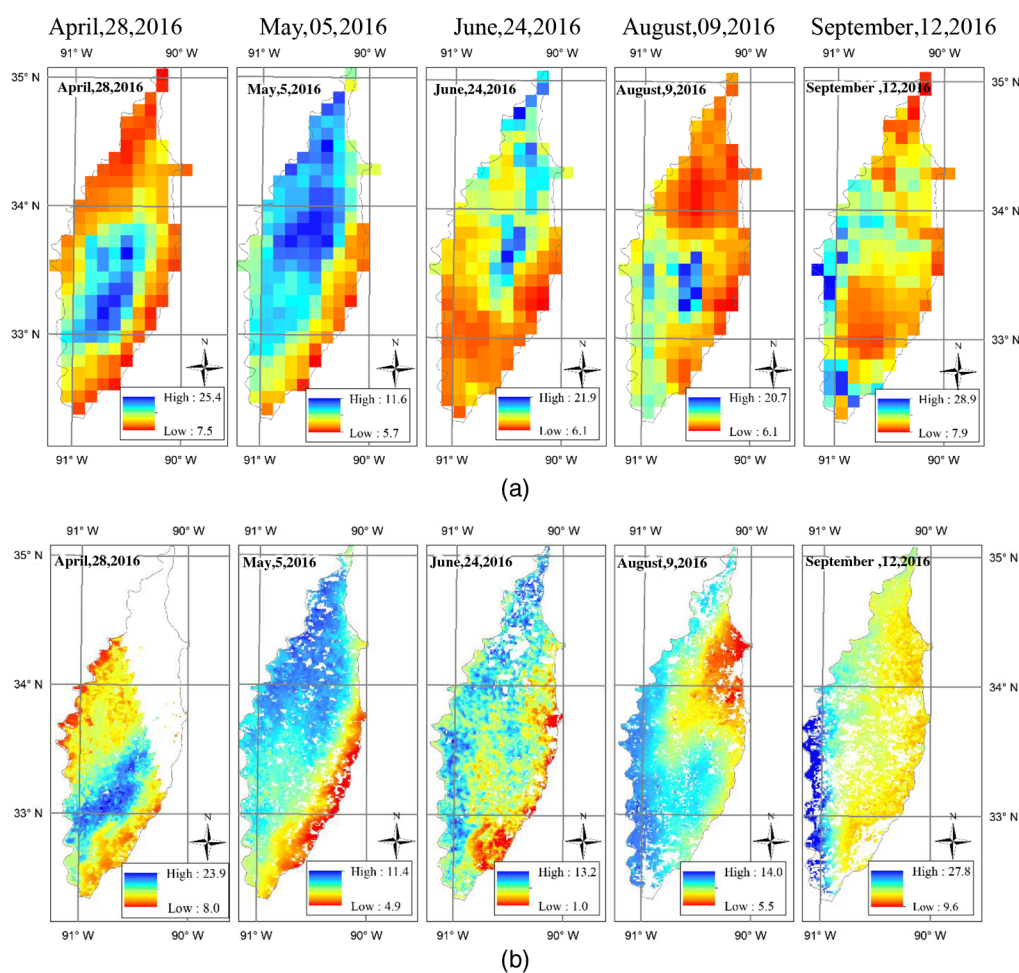


Fig. 4 (a) Volumetric soil moisture (%) maps of AMSR2 10-km-resolution products. (b) Volumetric soil moisture maps downscaled to 1-km resolution using modified universal triangle method.

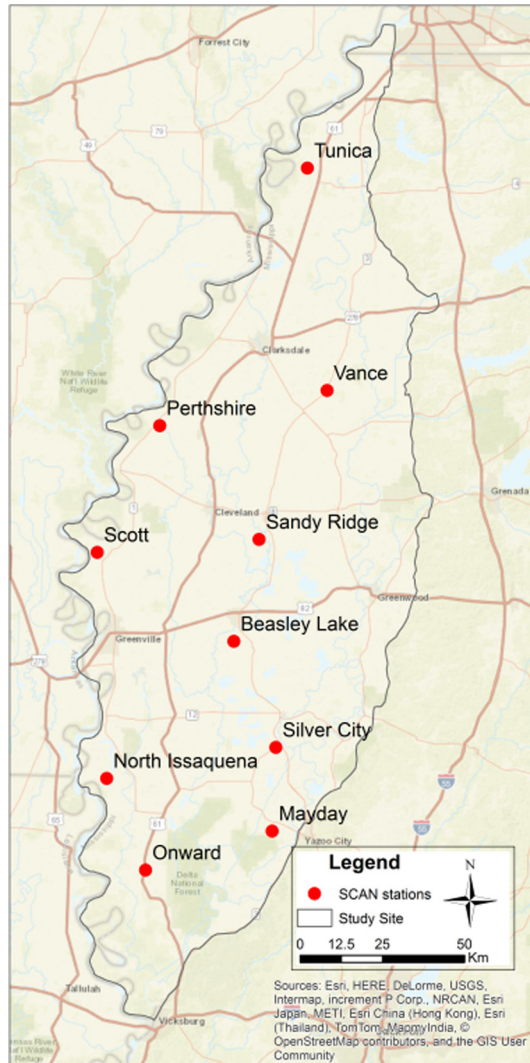


Fig. 5 SCAN network stations in the study site.

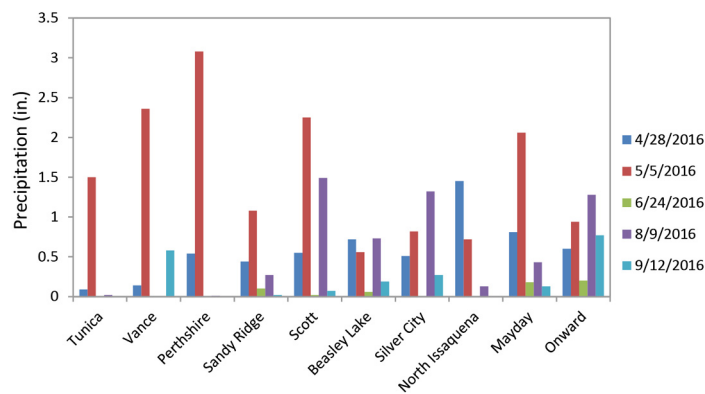


Fig. 6 Total precipitation increment in 5 days before each study date.³³

6 Accuracy Assessment

The accuracy of the results is assessed by comparison of the model predicted value and independently measured field soil moisture data. The mean absolute error (MAE) and root mean square error (RMSE) calculated from calibrated *in-situ* data are shown in Table 1. The MAE and RMSE for each study date are calculated from 33 data points and the total accuracy is calculated from all

Table 1 Accuracy results.

Error		April 28, 2016	May 5, 2016	June 24, 2016	August 9, 2016	September 12, 2016	Overall
AMSR2	MAE (%)	5.9	6.4	10.1	8.4	8.0	8.0
	RMSE (%)	6.7	8.3	11.6	11.5	9.0	9.7
Modified VI-LST model	MAE (%)	4.2	4.6	7.8	5.7	5.6	5.6
	RMSE (%)	4.5	5.6	7.9	6.6	6.4	6.5

165 data points. The overall MAEs and RMSEs of the modified VI-LST triangle method improved by 2.4% and 3.2%, respectively. The decrease in MAE and RMSE values indicate that the modified VI-LST triangle method improves the retrieval accuracy of AMSR2.

The results show that the MAE of the AMSR2 soil moisture even in a vegetated area such as Mississippi Delta is still below the 10.0% standard accuracy of the sensor. The accuracy obtained by the sensor over low-vegetated or semiarid regions, however, is significantly different. The AMSR2 2017 product update report shows that the soil moisture products have an average MAE of 3.54% over the semiarid areas of Murrumbidgee catchment in Australia and Ulaanbaatar in Mongolia.³⁹

The MAE and RMSE values for individual dates indicate that from April to June the error in the estimated soil moisture increases significantly and the error reaches its maximum in late June. The increase in MAEs and RMSEs is due to the increase in the vegetation height and density as the growing season progresses from April to June. Some crop types, such as soybeans and cotton, approach their maximum vegetation density in July. Thereafter, the error gradually decreases from June to September as the harvest season begins and AMSR2 observes more harvested and usually dry fields.

Table 2 shows the observed error classified by NDVI. The accuracy results confirm that the error in AMSR2-estimated soil moisture will increase with the increase in NDVI. The modified VI-LST model has improved the accuracy in all NDVI categories. Therefore, the downscaling model does not only reduce the overall bias, but it also actually reduces some of the biasing effects on LPRM caused by vegetation. The error in estimated soil moisture, however, still increases as the NDVI value increases.

The field observations data showed that AMSR2 can exceed its 10% standard accuracy when vegetation grows and mask the soil (Fig. 2). The *in-situ*-measured soil moisture data showed that as vegetation density increases, the increased emissivity due to vegetation⁴⁰ makes AMSR2 overestimate the soil moisture. Based on the data in Table 2, we concluded that for NDVI > 0.4 AMSR2 exceeds its 10% standard accuracy.

7 Conclusion

In this paper, AMSR2 soil moisture and BT data and VIIRS LST and VI Environmental Data Record data acquired simultaneously over agricultural fields were used in modified universal triangle model to improve the accuracy of soil moisture retrieval.

Table 2 Accuracy results in different NDVI intervals.

Error		NDVI < 0.2	0.2 < NDVI < 0.4	0.4 < NDVI < 0.6	0.6 < NDVI
AMSR2	MAE (%)	6.0	6.9	9.4	11.0
	RMSE (%)	7.0	8.3	11.0	14.1
Modified VI-LST model	MAE (%)	4.4	4.8	7.0	7.2
	RMSE (%)	5.3	5.4	7.4	7.4

To achieve the main objective of the study, ground observations were acquired simultaneously over various crop types during the growing season. The key issue in measuring soil moisture in vegetated agricultural environments is the masking of soil by vegetation cover and the emissivity of vegetation canopy. To address this concern, a modified universal triangle model was used to downscale the AMSR2 soil moisture product and improve the retrieval accuracy.

We found that soil moisture retrieval accuracy has an inverse relationship with the VI. The ground observations showed that AMSR2 overestimates soil moisture as NDVI value increases. The downscaling technique used in this study improved the accuracy over the vegetated areas by introducing the land surface parameters in the linking model and showed that the 5.0% goal accuracy for MAE is reachable for NDVI <0.4. The daily LST and VI data obtained by VIIRS provide a unique source of daily ancillary information that can be used to downscale AMSR2 soil moisture product to finer subkilometer resolution and improve the retrieval accuracy of soil moisture values in the presence of vegetation.

This downscaling method may be applicable for other areas with dominant vegetation land cover to improve the soil moisture retrieval accuracy using the daily surface temperature and VI data. The sensitivity of soil moisture data collection not only depends on NDVI and vegetation density, but it also depends on the types of crops, due to the characteristics of the crops such as orientation, leaf size and density, and water demand. Future work will focus on addressing this issue as the accuracy of the sensor could be better interpreted by various crop types and tillage practices.

Acknowledgments

The project described in this publication was supported by Grant No. G14AP00002 from the Department of the Interior, U.S. Geological Survey, to AmericaView. Its contents are solely the responsibility of the authors; the views and conclusions contained in this article are those of the authors and should not be interpreted as representing the opinions or policies of the U.S. government. Mention of trade names or commercial products does not constitute their endorsement by the U.S. government. This article is submitted for publication with the understanding that the U.S. government is authorized to reproduce and distribute reprints for governmental purposes.

References

1. S. I. Seneviratne et al., "Investigating soil moisture–climate interactions in a changing climate: a review," *Earth-Sci. Rev.* **99**(3), 125–161 (2010).
2. A. Xaver et al., "The potential of crowd sourced in situ soil moisture for environmental research," in *Proc. Conf. 20th EGU General Assembly, EGU2018*, p. 15602 (2018).
3. D. R. Legates et al., "Soil moisture: a central and unifying theme in physical geography," *Prog. Phys. Geogr.* **35**(1), 65–86 (2011).
4. M. S. Moran et al., "Estimating soil moisture at the watershed scale with satellite-based radar and land surface models," *Can. J. Remote Sens.* **30**(5), 805–826 (2004).
5. M. Owe and A. A. V. de Griend, "Comparison of soil moisture penetration depths for several bare soils at two microwave frequencies and implications for remote sensing," *Water Resour. Res.* **34**(9), 2319–2327 (1998).
6. T. J. Jackson, III, "Measuring surface soil moisture using passive microwave remote sensing," *Hydrol. Processes* **7**(2), 139–152 (1993).
7. C. Elachi and J. J. Van Zyl, *Introduction to the Physics and Techniques of Remote Sensing*, 2nd ed., John Wiley & Sons, Inc., Hoboken, New Jersey (2006).
8. F. T. Ulaby, R. K. Moore, and A. K. Fung, *Microwave Remote Sensing Active and Passive-Volume III: From Theory to Applications*, Artech House, Norwood, Massachusetts (1986).
9. M. P. Finn et al., "Remote sensing of soil moisture using airborne hyperspectral data," *GISci. Remote Sens.* **48**(4), 522–540 (2011).
10. J. Kolassa et al., "Soil moisture retrieval from AMSR-E and ASCAT microwave observation synergy. Part 1: satellite data analysis," *Remote Sens. Environ.* **173**, 1–14 (2016).

11. R. Prakash, D. Singh, and N. P. Pathak, "A fusion approach to retrieve soil moisture with SAR and optical data," *IEEE J. Sel. Top. Appl. Earth Obs. Remote Sens.* **5**(1), 196–206 (2012).
12. D. Thoma et al., "Comparison of four models to determine surface soil moisture from C-band radar imagery in a sparsely vegetated semiarid landscape," *Water Resour. Res.* **42**, 1–12 (2006).
13. T. Schmugge and T. Jackson, "Passive microwave remote sensing of soil moisture," in *EARSeL Adv. Remote Sens.*, pp. 5–14 (1993).
14. M. Owe, R. de Jeu, and J. Walker, "A methodology for surface soil moisture and vegetation optical depth retrieval using the microwave polarization difference index," *IEEE Trans. Geosci. Remote Sens.* **39**(8), 1643–1654 (2001).
15. X. Zhan, J. Liu, and L. Zhao, *Soil Moisture Operational Product System (SMOPS): Algorithm Theoretical Basis Document—Version 4.0*, NOAA NESDIS STAR, Suitland, Maryland (2016).
16. E. G. Njoku et al., "Soil moisture retrieval from AMSR-E," *IEEE Trans. Geosci. Remote Sens.* **41**(2), 215–229 (2003).
17. C. Notarnicola, M. Angiulli, and F. Posa, "Use of radar and optical remotely sensed data for soil moisture retrieval over vegetated areas," *IEEE Trans. Geosci. Remote Sens.* **44**(4), 925–935 (2006).
18. F. T. Ulaby, M. Razani, and M. C. Dobson, "Effects of vegetation cover on the microwave radiometric sensitivity to soil moisture," *IEEE Trans. Geosci. Remote Sens.* **GE-21**(1), 51–61 (1983).
19. D. J. Leroux et al., "Spatial distribution and possible sources of SMOS errors at the global scale," *Remote Sens. Environ.* **133**, 240–250 (2013).
20. V. Lakshmi, "Remote sensing of soil moisture," *Int. Scholarly Res. Not.* **2013**, 1–33 (2013).
21. C. Homer et al., "Completion of the 2011 National Land Cover Database for the conterminous United States—representing a decade of land cover change information," *Photogramm. Eng. Remote Sens.* **81**(5), 345–354.
22. M. Owe, R. de Jeu, and T. Holmes, "Multisensor historical climatology of satellite-derived global land surface moisture," *J. Geophys. Res. Earth Surf.* **113**, F01002 (2008).
23. "WaterScout SM100 soil moisture sensor product manual," Report No.: Item # 6460, Spectrum Technologies, Inc., http://www.especmic.co.jp/download/manual/WatchDog/6460_SM1001.pdf (2013).
24. ASTM International, *ASTM D 2216-98 Standard Test Method for Laboratory Determination of Water (Moisture) Content of Soil and Rock by Mass*, American Society for Testing and Materials, West Conshohocken, Pennsylvania (1999).
25. A. Griffin and Y. Yu, "VIIRS land surface temperature (LST) EDR release, validated stage 1 data quality," National Oceanic and Atmospheric Administration Joint Polar Satellite System, https://www.star.nesdis.noaa.gov/jps/documents/AMM/NPP/Land_LST_Validated_ReadMe.pdf (2015).
26. A. Griffin, M. Vargas, and T. Miura, "VIIRS vegetation index Environmental Data Record (VIIRS VI-EDR) release validated stage 1 data quality," National Oceanic and Atmospheric Administration Joint Polar Satellite System, https://www.star.nesdis.noaa.gov/jps/documents/AMM/NPP/Land_VI_Validated_ReadMe.pdf (2015).
27. NOAA CLASS data, "JPSS Visible Infrared Imaging Radiometer Suite Environmental Data Record (VIIRS_EDR)," 2016, <https://www.class.noaa.gov/>.
28. R. M. Parinussa et al., "A preliminary study toward consistent soil moisture from AMSR2," *J. Hydrometeorol.* **16**(2), 932–947 (2015).
29. Y. Inoue et al., "Season-long daily measurements of multifrequency (Ka, Ku, X, C, and L) and full-polarization backscatter signatures over paddy rice field and their relationship with biological variables," *Remote Sens. Environ.* **81**(2), 194–204 (2002).
30. E. Santi et al., "An algorithm for generating soil moisture and snow depth maps from microwave spaceborne radiometers: HydroAlgo," *Hydrol. Earth Syst. Sci.* **16**(10), 3659–3676 (2012).
31. J. Liu and X. Zhan, "Algorithm theoretical basis document: GCOM-W1/AMSR2 soil moisture product," NOAA Satellite Products and Services Review Board (2016).

32. F. Wentz et al., *Remote Sensing Systems GCOM-WI AMSR2 Daily Environmental Suite on 0.1 Deg Grid Version 7.2*, Remote Sensing Systems, Santa Rosa, California (2014).
33. "Soil climate analysis network data," National Resources Conservation Service—United States Department of Agriculture, 2016, <https://www.wcc.nrcs.usda.gov/scan/>.
34. T. N. Carlson, R. R. Gillies, and E. M. Perry, "A method to make use of thermal infrared temperature and NDVI measurements to infer surface soil water content and fractional vegetation cover," *Remote Sens. Rev.* **9**(1), 161–173 (1994).
35. A. K. M. Hossain, "Developing a virtual sensor (VS) for mapping soil moisture at high spatial and temporal resolution," Thesis, The University of Mississippi (2008).
36. T. Carlson, "An overview of the 'triangle method' for estimating surface evapotranspiration and soil moisture from satellite imagery," *Sensors* **7**(8), 1612–1629 (2007).
37. M. Piles et al., "Downscaling SMOS-derived soil moisture using MODIS visible/infrared data," *IEEE Trans. Geosci. Remote Sens.* **49**(9), 3156–3166 (2011).
38. I. Markovsky and S. Van Huffel, "Overview of total least-squares methods," *Signal Process.* **87**(10), 2283–2302 (2007).
39. "AMSR2 products update," Report No.: Version 3.0, pp. 15–17, JAXA Earth Observation Research Center, 2017, https://suzaku.eorc.jaxa.jp/GCOM_W/materials/product/170222_Ver3.0_release_e.pdf.
40. A. Olioso et al., "Evidence of low land surface thermal infrared emissivity in the presence of dry vegetation," *IEEE Geosci. Remote Sens. Lett.* **4**(1), 112–116 (2007).

Saeed Arab is a remote sensing data scientist at the U.S. Geological Survey (USGS) Earth Resources Observation and Science Center. Formerly having been trained in geomatics engineering and geospatial science, Saeed earned a PhD in geological engineering from University of Mississippi in 2018. His current role includes characterization and validation of new remote sensing science products to support their use in an operational environment.

Gregory L. Easson is a professor at the University of Mississippi's Department of Geology and Geological Engineering and a director of Mississippi Mineral Resources Institute. He obtained his PhD in 1996 from the University of Missouri at Rolla. He received his MSc degree from the University of Missouri and his BSc degree from Southwest Missouri State University. Prior to his academic work at the University of Mississippi, he worked for the USGS and the Missouri Department of Natural Resources. His research at Ole Miss focused on the various aspects of remote sensing and geographical information system development.